

## Mode Control for Emerging Link Performance Standards

A.G.Hallam<sup>1,3</sup>, D.A.Robinson<sup>2</sup>, I.Bennion<sup>1</sup>

<sup>1</sup>The Photonics Research Group, Aston University, Birmingham, B4 7ET, U.K.

<sup>3</sup>Permanent address: 'Sandridge', Winchester Road, Waltham Chase, Hampshire, SO32 2LG, U.K.

<sup>2</sup>Arden Photonics Ltd., iBIC, Holt Court Rd, Aston Science Park, Birmingham, B7 4EJ, U.K.

**Abstract:** A novel mode control device is described, comprising a point-load mode-scrambler in tandem with a mode-filter. The device may be tuned to ensure compliance of fibre test equipment with new link performance standards. Improvement in the reproducibility of insertion loss measurements on concatenated fibres is demonstrated.

### 1 Introduction

Emerging standards for 1Gb/s and 10Gb/s Ethernet transmission over multimode optical fibre have led to a resurgence of interest in the precise control and specification of modal launch conditions. In particular, ISO/IEC14763-3 [1] and IEEE802.3 [2] specify modal launch in terms of the Mode Power Distribution [3] and Encircled Flux [4], respectively. Commercial LED and OTDR test equipment does not, in general, comply with these standards and so there is a need for mode control devices to enable test sets to comply with the standards. A novel mode control device, comprising a mode-scrambler operating in tandem with a mode-filter, is described. An example of the improvement in loss measurements, resulting from the use this device, is demonstrated by measuring the insertion loss of a series of concatenated patchcords with a range of different launch conditions.

### 2 Mode-Scramblers

A variety of mode-scrambling techniques has been described in the literature, such as sinusoidal bending [5], devitrification [6] and microbending [7], applied to step-index fibres, and Long Period Gratings (LPGs) [8], etched fibre ends [9], and offset launch [10], applied to graded-index fibres. In the case of a step-index mode-scrambler it is necessary to provide some additional mode-filtering in

the target graded-index fibre to achieve the required modal filling. There is an advantage, therefore, in providing the required amount of mode-conditioning directly to the graded-index fibre and there are devices on the market designed to do this, which work by mechanically impressing an LPG on the fibre. To test this method, an LPG was constructed consisting of a bed of seven contacting pins, each of

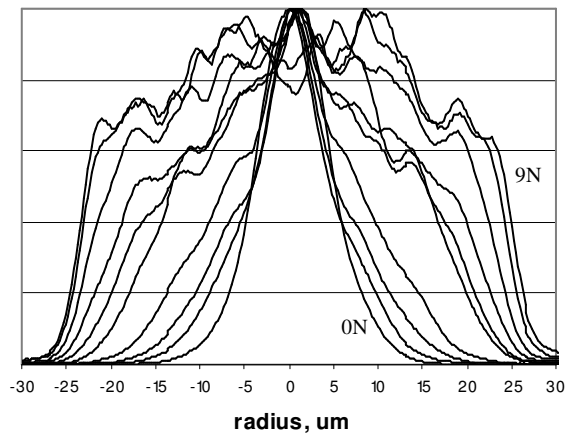


**Fig. 1** Near-field profiles of a 50µm graded-index fibre in an LPG as the grating load was increased from zero to 9N.

1mm diameter. A 50µm graded-index fibre was positioned across the pins and pressed against them with a soft former, causing the fibre to take up the period of the grating. The fibre was illuminated with light at 850nm from a singlemode fibre and the output intensity distribution of was measured using a video microscope. The normalised near-field profiles, shown in Fig. 1, show that light was progressively coupled to higher-order modes, characterised by increased width of the near-field, as the grating load was increased from zero to 9N. The distribution did not, however, approach that corresponding to the roughly triangular shape, corresponding to an Equilibrium Mode Distribution [11], or to a parabolic shape, corresponding to a fully-filled distribution. The reason for this is that the difference in propagation constant  $\Delta\beta$  between all adjacent mode groups in a graded-index fibre is constant, so the LPG progressively couples light from the lowest-order modes to the higher-order modes and eventually to leaky and radiative modes, resulting in a squarish distribution. This device is thus not suitable for producing the finely-tuned mode distributions that are required for the new standards. The approach taken here is, therefore, to apply a combination of a mode-scrambler in series with a mode-filter to enable flexibility and tuning of the modal distribution.

The mode-scrambler consists of bending a fibre round in a loop such that it crosses back over itself, and applying a load to the crossover point. In this manner, each fibre section acts as a source of point loading for the other. The resultant distortion to the fibre leads to a wide spectrum of spatial frequencies in the fibre. This is a particular advantage for mode coupling in step-index fibres, where adjacent modes are not evenly spaced. For example, in a typical 50µm step-index fibre at 850nm, the

difference in  $\Delta\beta$  between adjacent modes varies from  $1.5 \times 10^{-3} \text{ rad.mm}^{-1}$  to  $2.5 \text{ rad.mm}^{-1}$ . In contrast, for a  $50\mu\text{m}$  graded-index fibre the 19 possible mode-groups, each consisting of a number of degenerate modes, have almost identical spacing at  $5.9 \text{ rad.mm}^{-1}$ .

The crossover point is sandwiched between two jaws of elastic material, shown in Fig.2, such that application of a compressive force to the structure causes fibre sections A and B to be pressed into the jaws. A particular feature of this device is that it can be tuned in real-time by adjusting the applied force

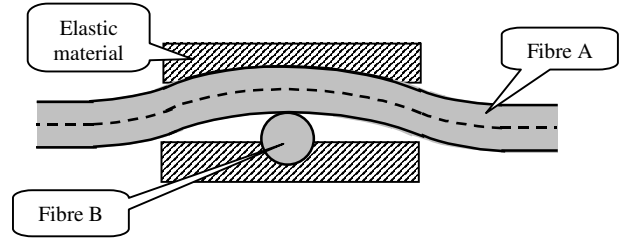


**Fig. 2** Schematic of crossover in point-load mode-scrambler with silica fibre and elastic compression jaws.

whilst monitoring the output of the fibre. A further advantage is that point loading is applied equally to the fibre at two longitudinal positions, one loop-length apart, leading to a more complete mode scrambling. The distortion of the fibre may be calculated using bending beam theory as follows. From Roark [12], the displacement  $y(z)$  of a concentrated load  $W$  applied to an infinite beam on an elastic foundation, as a function of axial distance  $z$ , is given by

$$y(z) = -\frac{W}{8EI\phi^3} e^{-\phi z} (\cos \phi z + \sin \phi z) \quad (1)$$

$$\text{where: } \phi = \left( \frac{b_o k_o}{4EI} \right)^{1/4} \quad (2)$$

and  $E$ ,  $I$  and  $b_o$  are Young's modulus, the moment of inertia and the width of the beam, respectively, and  $k_o$  is the foundation modulus (unit stress per unit deflection) [13]. The displacement of each individual fibre is equal to one-half of the displacement calculated from (1), as both jaws are compressed equally.

It is known [14] that the coupling strength between modes is proportional to the curvature spectrum of the fibre. The local fibre curvature  $c(z)$  is given by [15],

$$c(z) = \frac{y''(z)}{(1 + y'(z)^2)^{3/2}} \quad (3)$$

For a given fibre, the shape of the curvature spectrum depends on the Young's moduli of the fibre and the jaw materials, and its amplitude depends on the applied load. Thus selection of the jaw material, and the applied load, can be used to achieve a high degree of tuning.

As an example, consider a dual-coated silica fibre with Young's modulus values of 72GPa, 10MPa and 1.3GPa for the cladding, inner coating, and outer coating respectively. Taking an area-weighted mean of the three materials gives an average Young's modulus of 18GPa. Choosing, for example, polypropylene with Young's modulus 1.3GPa, for the jaw material, and a load of 5N, the curvature spectrum from (3) is shown in Fig. 3(a). Also shown is a histogram of the frequency spectrum for coupling between adjacent fibre modes for a step-index fibre and a graded-index fibre. It can be seen that there is a significant overlap between the curvature spectrum and the spectrum of the graded-index fibre, but much less for the step-index fibre.

Fig. 3(b) shows the respective spectra for coupling between all the modes, both adjacent and non-adjacent. Here, there is a high degree of overlap for the step-index fibre, indicating that the device should provide a high degree of mode-scrambling for this type of fibre.

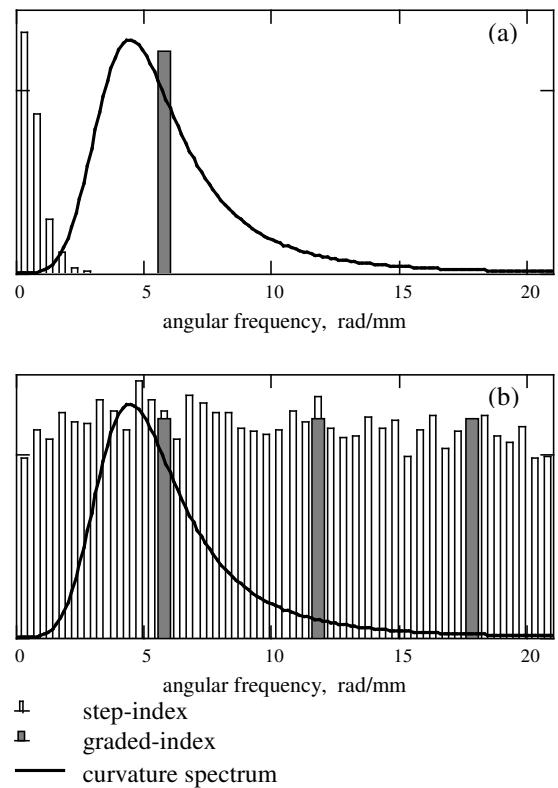


**Fig. 3** Curvature spectrum of point-load mode-scrambler, and  $\Delta\beta$  spectrum for coupling between modes in step and graded-index fibres: (a) adjacent modes, (b) all modes.

A practical implementation of the loop mode-scrambler was constructed by forming a loop in the fibre and passing the end back through the loop. In this way a stable loop of approximately 20mm diameter could be formed. In this configuration there

are three crossover points situated in close proximity. The crossover points were located between two rigid

jaws, each lined with a 400 $\mu$ m thick film of polypropylene, and a compressive force applied. The near-field intensity profiles at the output of the mode-scrambler were measured as a function of applied load for an underfilled launch, shown in Fig. 4. It was found that even for zero loading there

was a degree of natural mode-scrambling occurring. The flat topped profile occurring at 4N indicated that the fibre modes were all equally excited. Increasing the load further caused a slight bias towards higher-order and leaky modes, identified by the concave shape. Note that, for clarity, the curves have been normalised and offset vertically. The output of

the point-load device was then spliced to a 50 $\mu$ m graded-index output fibre and the Mode Power Distribution (MPD) was measured. The results,

plotted in Fig. 5, show that for zero loading a singlemode launch clearly underfills the graded-index fibre. The MPD was computed using the measured refractive index profile of the fibre as the reference profile [3], and so a fully-filled distribution would correspond to a diagonal line from the lower left to the top right corner. When a load of 6N was applied, however, the MPDs for both launches converge to give a stable, fully-filled, mode distribution.

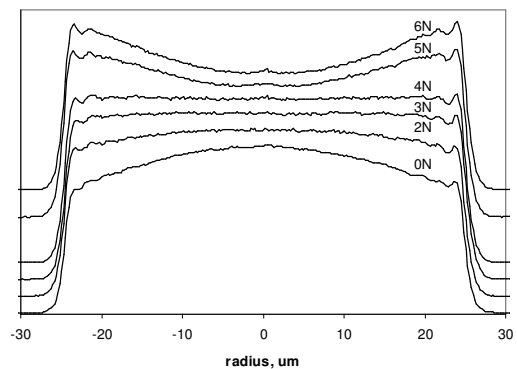


**Fig. 4** Near-field profiles of 50 $\mu$ m step-index fibre vs point loading.

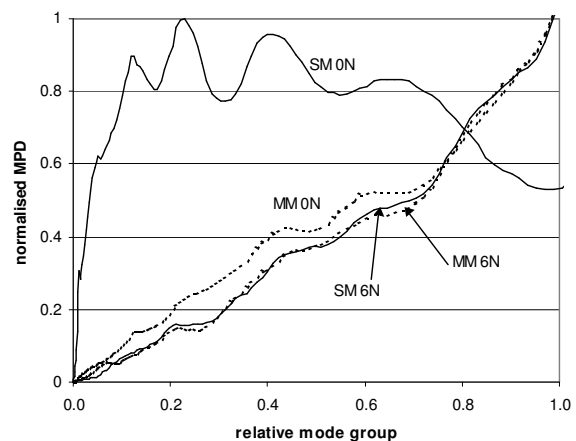


**Fig. 5** Measured MPDs of graded-index fibre spliced to point-load mode-scrambler, for singlemode (solid) and multimode (dotted) launches.

### 3 Mode Filters

In order to tune the mode distribution, the mode-scrambler was tested in series with two types of mode

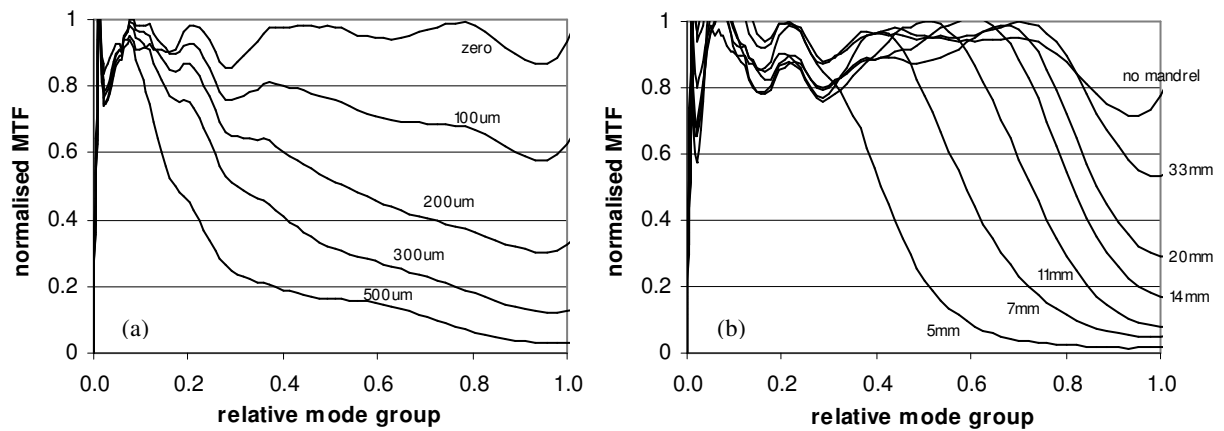


**Fig. 6** MTFs of (a) longitudinal filter, vs air gap, and (b) mandrel-wrap filter, vs mandrel diameter.

filter, a longitudinal gap filter and a mandrel-wrap filter. The longitudinal gap filter consisted of a small air gap between two sections of step-index fibre, positioned immediately after the mode-scrambler. The principle of the filter is that overlap of the higher order-modes from the source fibre with the target fibre becomes progressively less as the gap is increased. Fig. 6(a) shows a series of Mode Transfer Function (MTF) curves as the gap is increased from zero to 500 $\mu$ m. For zero gap in the filter the MTF is essentially unity value for all modes, indicating a fully-filled distribution. As the gap is increased, the MTF is attenuated in a manner roughly proportional to the mode group number.

The mandrel-wrap mode-filter consisted of a single loop in the graded-index fibre around a mandrel. Fig. 6(b) shows the MTFs for a range of mandrel diameters, from essentially straight, down to 5mm. For this filter, the MTF remained effectively unity up to a 'knee' position, where a roll-off in the higher mode groups occurred. The position of the knee shifted to the left, as the mandrel diameter was reduced. The corresponding encircled flux plots for these filters are shown in Fig. 7. As the gap in the air-gap filter is increased, the curves become steeper around the mid-radius position but converge towards the edge of the core. In contrast, the mandrel-wrap mode-filter predominantly affects the higher-order modes, towards the core boundary, which are progressively attenuated as the bend diameter is reduced. By using a combination of the two types of filter it is possible to produce a range

of encircled flux profiles to suit particular standards requirements.

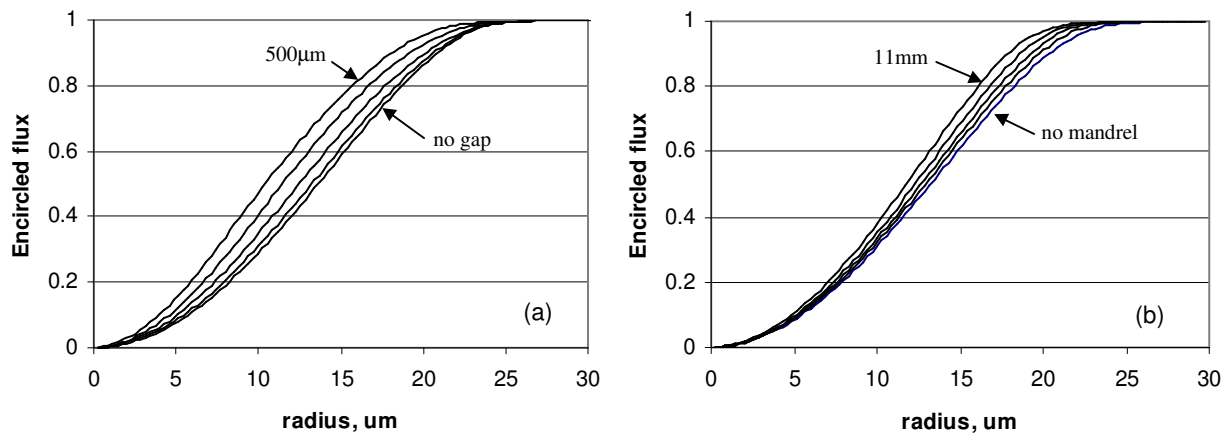


**Fig. 7** Encircled flux of (a) longitudinal filter, vs air gaps of zero, 100 $\mu\text{m}$ , 200 $\mu\text{m}$ , 300 $\mu\text{m}$ , 500 $\mu\text{m}$ , and (b) mandrel-wrap filter, vs mandrel diameters of no mandrel, 33mm, 20mm, 14mm, 11mm.

#### 4 Wavelength Sensitivity

Many commercial dual-wavelength LAN testers employ a means of combining the output from two sources at different wavelengths into common output connector. This arrangement clearly speeds up the measurement process, and assists in automation, but it is also important to achieve standards compliance at both wavelengths. To test the wavelength sensitivity of the mode control techniques described above, two devices were assembled with 50 $\mu\text{m}$  and 62.5 $\mu\text{m}$  output fibres, each comprising a point-load mode-scrambler and a mandrel-wrap mode-filter of one half turn of 30mm diameter. The

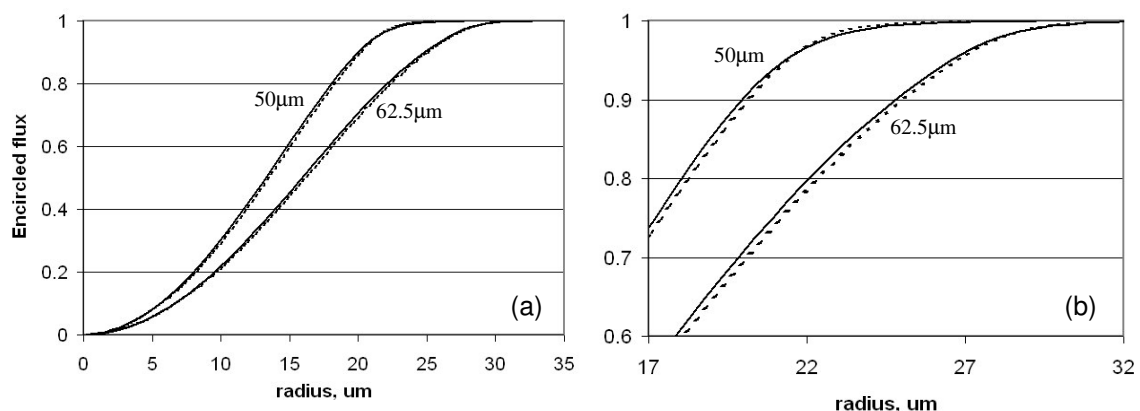


**Fig. 8** Measured encircled flux at 850nm (dotted) and 1300nm (solid) for 50 $\mu\text{m}$  and 62.5 $\mu\text{m}$  mode control devices, (a) full curve, (b) magnified view.

encircled flux was then measured at 850nm and 1300nm and the results are shown in Fig. 8. The

encircled flux at 1300nm is slightly to the left of that at 850nm for most of the radius, and also that the two curves cross over at a position near to the core boundary, at about 22µm radius for the 50µm fibre. It can be shown [16] from theoretical Laguerre-Gauss solutions of parabolic-index fibres that this behaviour may be expected and is due to the occurrence of a slightly longer evanescent tail in the cladding at 1300nm.

**5 Applications of Mode Control**

A practical mode controller was built, consisting of a point-load mode-scrambler in tandem with a mandrel wrap mode-filter, shown schematically in Fig. 9. The step-index input fibre is formed into a 20mm diameter loop and pressure applied to the crossover points of the fibre by means of a pinch plate. The step-index fibre was spliced to a graded-index output fibre and was formed into a single half-turn of approximately 30mm diameter. By means of adjusting the pressure on the pinch plate and the diameter of the bend in the graded-index fibre, the output modal distribution was adjusted to comply with the IEC/ISO14763-3 standard. Fig 10 shows a fully ruggedised style of the mode controller for field use.

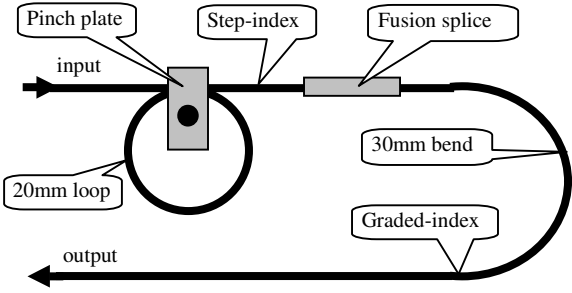


**Fig. 9** Schematic of mode controller



**Fig. 10** Photograph of ruggedised mode controller.

To test the performance of the mode controller, a concatenated link of eleven 50µm patchcords was assembled, consisting of 3m fibre lengths and a mixture of ST, SC and FC connectors. The insertion loss of the link was measured using a variety of light sources including a singlemode launch, a commercial LAN tester, a mode-scrambler and an offset singlemode launch. The loss values, shown in Fig. 11, vary from 0.5dB, for the singlemode launch, to 5.1dB for the offset launch. The experiment

was then repeated with the mode control device positioned, in turn, between each source and the link under test. The measured range of losses was reduced from 4.6dB, without the mode controller, to 0.2dB with it, indicating a great improvement in reproducibility. The MPD of each of the sources was then

measured, shown in Fig. 12(a), and also the MPD after the mode controller was fitted, in Fig. 12(b).

The areas marked by dotted lines in the top corners, and lower centre, correspond to the MPD template specified in the ISO/IEC14763-3 link testing standard.

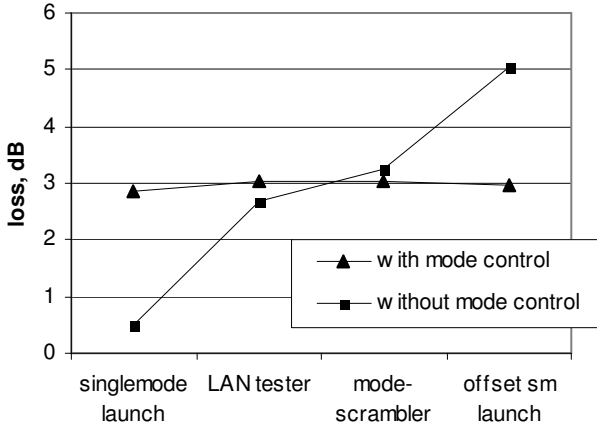


**Fig. 11** Insertion loss of eleven concatenated patchcords

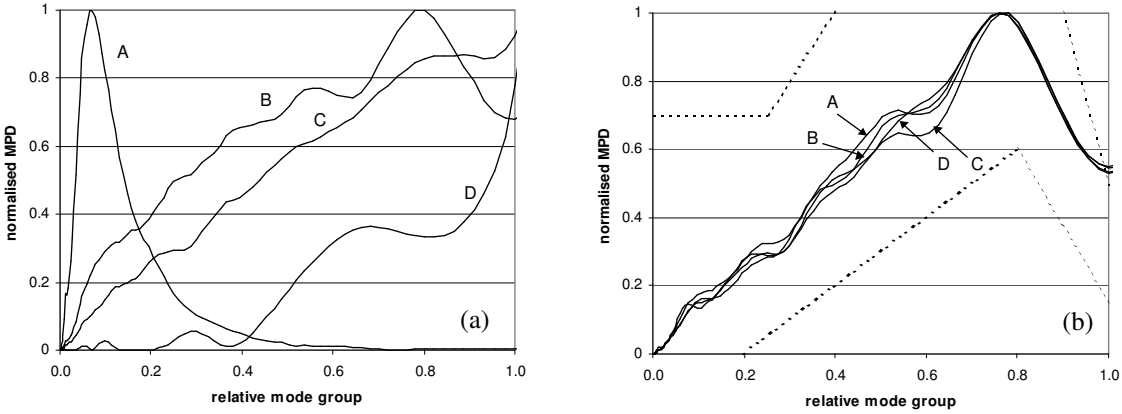


**Fig. 12** Measured MPDs, (a) direct from source, (b) after mode controller. A: singlemode launch, B: LAN tester, C: mode-scrambler, D: offset singlemode launch. The dotted lines show the ISO/IEC14763-3 MPD template.

IEC standard IEC61280-4-1 [17] specifies launch conditions in terms of upper and lower tolerances of the encircled flux distribution at different radial positions. By using the point-load mode-scrambler in tandem with a mandrel-wrap mode-filter, it was possible to produce an encircled flux profile to comply with the standard, shown in Fig. 13. Both a singlemode launch and a multimode launch were tested, demonstrating the insensitivity of the device to the launched distribution.

## 6 Summary

The use of mode control techniques to enable commercial test equipment to achieve compliance with international standards has been described. A novel point-load mode-scrambler operating in series with air-gap, and mandrel-wrap, mode-filters was shown to be able to produce a variety of mode power distributions and encircled flux profiles. In particular, compliance with launch requirements in link testing standards was achieved.

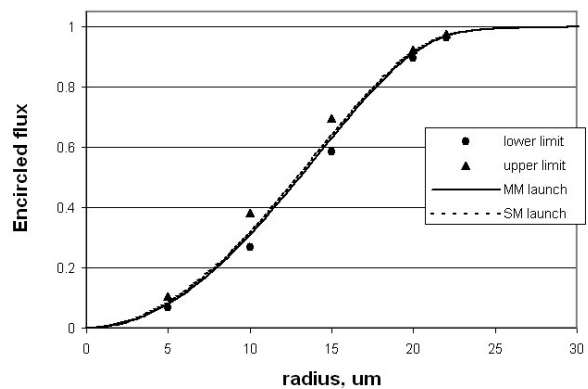


**Fig. 13** Measured encircled flux from mode controller and the encircled flux template from draft IEC61280-4-1.

Improvement in the reproducibility of insertion loss measurements on concatenated patchcords was demonstrated by inserting the device between a variety of test sources and the fibre under test. The mode control device showed very low sensitivity to launched distribution and was able to achieve standards compliance at both 850nm and 1300nm.

## 7 References

1. ISO/IEC14763-3, 'Information technology — Implementation and operation of customer premises cabling — Part 3: Testing of optical fibre cabling', 2006.
2. IEEE 802.3-2005, 'Information Technology - Telecommunication & Information Exchange Between Systems - Local and Metropolitan Area Networks - Specific Requirements, Part 3: Carrier Sense Multiple Access with Collision Detection (CSMA/CD) Access Method and Physical Layer Specifications', and amendment 802.3aq (2006).
3. IEC PAS61300-3-43. 'Examinations and measurements –Modal Distribution Measurement for fibre optic sources', 2006, 1<sup>st</sup> edn.
4. TIA/EIAFOTP-455-203, 'Launched Power Distribution Measurement Procedure for Graded-Index Multimode Fiber Transmitters', June 2001.
5. Tokuda, M., Seikai, S., Yoshida, K., and Uchida, N.: 'Measurement of baseband frequency response of multimode fibre by using a new type of mode scrambler', *Electron. Lett.*, 1977, **13**, (5), pp. 146-147.
6. Schlager, J.B., and Rose, A.H.: 'Annealed optical fibre mode scrambler', *Electron. Lett.*, 2001, **37**, (1), pp. 9-10.
7. Ikeda, M., Murakami, Y., and Kitayama, K.: 'Mode scrambler for optical fibers', *Appl. Opt.*, 1977, **16**, (4), pp. 1045-1049.
8. Su, L., Chiang, K.S., Lu, C.: 'Microbend-induced mode coupling in a graded-index multimode fiber', *Appl. Opt.*, 2005, **44**, (34), pp. 7394-7402.
9. Ikeda, M., Sugimura, A., and Ikegami, T.: 'Multimode optical fibers: steady state mode exciter', *Appl. Opt.*, 1976, **15**, (9), pp. 2116-2121.
10. Raddatz, L., White, I.H., Cunningham, D.G., and Nowell, M.C.: 'An experimental and theoretical study of the offset launch technique for the enhancement of the bandwidth of multimode fiber links', *IEEE J. Lightwave Technol.*, 1998, **16**, (3), pp. 324-331.
11. Yamashita, K., Koyamada, Y., and Hatano, Y.: 'Launching condition dependence of bandwidth in graded-index multimode fibers fabricated by MCVD or VAD method', *IEEE J. Lightwave Technol.*, 1985, **3**, (3), pp. 601-607.

12. Young, W.C., and Budynas, R.G.: 'Roark's Formulas Formulas for Stress and Strain', (McGraw-Hill, 2002, 7th edn.)
13. Olshansky, R.: 'Distortion Losses in Cabled optical Fibers', *Appl. Opt.*, 1975, **14**, (1), pp. 20-21.
14. Marcuse, D.: 'Coupled mode theory of round optical fibers', *Bell Syst. Tech. J.*, 1973, **52**, (6), pp. 817-842.
15. Borowski, E.J., and Borwein, J.M.: 'Dictionary of Mathematics', (Harper Collins, 1989, 1<sup>st</sup> edn.)
16. Hallam, A.G.: 'Mode Control in Multimode Fibre and its Applications', PhD Thesis, Aston University, 2007.
17. IEC 61280-4-1, 'Installed cable plant – Multimode attenuation measurement', Committee Draft 2007.